

Version-1

State of the Art H.E.L.P. Apheresis: Advances in Management of COVID-19, Long COVID, and Post-COVID-19 Vaccination Syndrome

Beate Roxane Jaeger^{1*}, Abdul Mannan Baig¹, Renata Linkesch², Dietrich Seidel³, Julian Douves¹, Sergio Presbitero Espinosa¹, Martin Rössner¹, Peter Holzhauer¹, Friedrich Migeod¹, Joachim Gerlach³, Martin Kräter^{4,5}, Jochen Guck⁴, Nikolaus Wick⁶, Hans Rausch⁷, Anne McCloskey, Sandy Rosko, Usman Ali,

¹Clinic St Georg, Bad Aibling, Germany

²B.Braun Medical Care, Zürich, Switzerland

³Health-Shield, Vedicinals-9, 40764 Langenfeld, Germany

⁴Biotechnology Center, Center for Molecular and Cellular Bioengineering, Technische Universität Dresden, Dresden, Germany

⁵Medical Clinic I, University Hospital Carl Gustav Carus, Technische Universität Dresden, Dresden, Germany

⁶Speziallabor Wick, Innsbruck, Austria

⁷Naturwerk GmbH&CoKG, Bavaria, Germany

⁸Directorate of Respiratory Medicine, Northwest Lung Centre, Manchester University Hospitals NHS Trust, Wythenshawe Hospital, Manchester, United Kingdom

⁹School of Medicine, Faculty of Medicine, Biology and Health, The University of Manchester, Oxford Road, Manchester, United Kingdom

* Correspondence:

Dr. Med. Beate Roxane Jaeger
Head of the Department of H.E.L.P. Apheresis

Short title:

H.E.L.P. Apheresis: Advances in Treatment of COVID-19-Related Hypercoagulability Syndrome

Abstract

Over the past three years, the practice of H.E.L.P. apheresis has faced the daunting challenge of managing hypercoagulable states in COVID-19 and Long COVID. Due to the association of multiple organ damage in COVID-19 and Long COVID with endothelial injury, procoagulant factor dominance, and ischemia-induced tissue injury, H.E.L.P. apheresis has distinctly demonstrated its advantage. It effectively lowers plasma levels of clotting factors, the spike protein, toxins, cytokines, and harmful lipids, thereby mitigating disease-related morbidity and mortality during the ongoing pandemic. Here, we provide compelling evidence showcasing the distinctive efficacy of this therapeutic modality both with and without anticoagulation drug therapy. This approach has proven beneficial for a significant cohort of patients experiencing Long COVID and ME/CFS, addressing their needs across both the active and chronic phases of the disease. With the increasing prevalence of post-COVID-19 vaccination syndrome patients, H.E.L.P. apheresis has attained a new modality of significance to help this group of sufferers, in addition to the COVID-19 and Long COVID categories.

1. Introduction

As a result of the COVID-19 pandemic, the scientific community is challenged with pinpointing a specific treatment approach suitable for individuals experiencing both acute and chronic manifestations of the virus, commonly referred to as 'Long COVID.' Preventing acute lung failure, which arises from so-called 'microthrombi' and endothelial inflammation (1,2), is challenging due to an excessive immune response when the body's initial defense mechanisms have already faltered. Therefore, a holistic treatment approach is imperative to address the intricate interplay of these mechanisms.

It is known that the SARS-CoV-2 spike (S) protein uses the angiotensin-converting enzyme 2 (ACE2) receptor and the transmembrane serine protease 2 (TMPRSS2) as essential host proteins (3,4,5) to infect cells of the alveolar epithelium (6–9) and endothelial cells in the lungs, heart, kidneys, intestines, liver, and brain (10). This explains why patients with an upregulated receptor density, such as patients with coronary artery disease (11–15), hypertension (8,15), diabetes (8,15), or obesity (8,15), exhibit a higher mortality risk (16). This problem has become increasingly complex with the discovery of other receptors being able to facilitate viral entry into the cells (17). Histological studies have confirmed the presence of the virus in the primary affected tissue in the lungs, specifically in cell types such as alveolar type I and II epithelium, as well as basal endothelial cells (6–9, 18). Moreover, these inflammatory comorbidities further increase thrombogenicity and hyperactivate platelets by increasing the shear stress in the vessels (19-21). Alveolar tissue and adjacent capillaries have revealed massive inflammatory infiltrates and procoagulant activation, together with cell necrosis, thrombi, and massive 'fibrinoid' deposits (6–9,18,22,23). As a result of this, the clinical picture of an obstructed gas exchange emerges in the patients admitted with acute COVID-19 in hospitals, as the thickening of the diffusion barrier limits the benefits of artificial ventilation and extracorporeal membrane oxygenation (ECMO) (24-27). The identification of the S protein in circulation following COVID-19 vaccination has further complicated the challenge of choosing an appropriate treatment modality for individuals experiencing cardiovascular (CVS) adverse events post-vaccination (28-30). Therefore, over the past three years, the selection of therapy to extend beyond acute COVID-19 to encompass Long COVID and emerging instances of vaccine-related cardiovascular adverse effects has become increasingly intricate (31).

Heparin-induced extracorporeal LDL/fibrinogen precipitation (H.E.L.P.) apheresis is a therapeutic procedure introduced by Seidel and Wieland in 1984, primarily for patients with severe hyperlipidemia or familial homozygous hypercholesterolemia (28-30,32-35). This therapy uses unfractionated heparin in the extracorporeal circuit to significantly contribute to the restoration of microcirculation in the lungs and other affected organs. H.E.L.P. apheresis has not only been proven beneficial as an ultima ratio treatment of arteriosclerosis and its atherothrombotic sequelae, but it has also been successfully applied in coronary heart disease (28,29,32,36-38) to prevent and treat graft vessel disease following heart transplantation (38-44), acute thrombotic graft occlusion following aortocoronary bypass surgery (45), preeclampsia (46,47), strokes (48-51), unstable angina pectoris (52), and hyperlipoproteinemia (a) (37). Various types of harmful lipoproteins and lipids are filtered out of circulation during H.E.L.P. apheresis. H.E.L.P. apheresis has also been shown to exert an anti-inflammatory effect in chronic and acute inflammatory processes involving the endothelium in the micro- and macro-circulation (29–30, 32-40,45,53,54), as well as anticoagulant and anti-inflammatory influences (55,56).

Furthermore, unfractionated heparin used in H.E.L.P. apheresis can effectively bind to the S protein, thereby mitigating endothelial injury, hypercoagulability, and thrombus formation triggered by the SARS-CoV-2 S protein and consequent sluggish circulation (28,55,56). Owing to this quality, individuals experiencing adverse CVS effects after mRNA COVID-19 vaccinations may be considered potential candidates for H.E.L.P. apheresis. At present, there is no drug-based therapy to engage and remove the S protein from those suffering from these patient groups, suggesting H.E.L.P. apheresis may be a potential therapy arsenal to help individuals who have a sustained production of S protein after a COVID-19 infection or vaccination. Additionally, the removal of harmful lipoproteins and lipids means that patients with additional inflammatory comorbidities would obtain additional health benefits from this type of apheresis (28,55,56).

The true impact of H.E.L.P. apheresis benefits can be assessed through two key parameters: a) the clinical enhancement observed in patients' post-procedure, and b) the amelioration of biomarkers that were dysregulated before the treatment was administered. With regards to the signs and symptoms of the patients undergoing H.E.L.P. apheresis, a checklist of CVS and non-CVS related clinical presentations should be considered, as H.E.L.P. apheresis is also able to reduce well-known 'neuro-COVID-19' symptoms (51-53). Though the cardinal biomarkers are described in detail in the following sections, it is important to mention that the

list should not be exhaustive and is central to the causation of hyper viscosity and endothelial injury. There is also potential that H.E.L.P. apheresis could help uncover the covert pathophysiology mechanisms underlying many diverse conditions that are not yet understood, including COVID-19, Long COVID, and Myalgic Encephalomyelitis/Chronic Fatigue Syndrome (ME/CFS). We have observed significant clinical benefits from applying H.E.L.P. apheresis, and it is crucial to communicate and share these advantages. This will facilitate the integration of this modality into patient treatment plans, enabling researchers and clinicians to advance in our collective effort to combat SARS-CoV-2 during the ongoing pandemic.

2. Material and Methods

2.1. The H.E.L.P. apheresis method

During H.E.L.P. apheresis, the blood cells are first separated from the plasma in an extracorporeal circuit. Following this, 400,000 units of unfractionated heparin are added to the plasma, and the pH is lowered to 5.12 using an acetate buffer. This is the isoelectric point for optimal precipitation of the apolipoproteins from LDL cholesterol, lipoprotein (a) [Lp (a)], and VLDL, which are precipitated in the precipitation filter together with fibrinogen. The excess heparin is adsorbed, and bicarbonate dialysis balances the pH again. The blood cells of the patients are reinfused in parallel with a saline solution (32,55). The duration of treatment, two hours on average, can be shortened or extended to meet individual needs (55).

2.2. Clinical testing before and after H.E.L.P. apheresis

Participants underwent a program of functional and physiological testing before and within 24 hours of H.E.L.P. apheresis. The clinical evaluations that were performed and their frequency are listed in Table 1. The tests were performed by trained volunteers assisting the treating physician (BRJ) and the nursing staff at the center.

In the week before arrival, patients completed the following assessments remotely:

- A detailed symptom and function checklist based on the modified COVID-19 Yorkshire Rehabilitation Screen (C-19 YRS) (57,58)
- A baseline cognitive assessment was performed using a computerized cognitive battery (BrainCheck; Houston, Texas). The six measures that make up the cognitive battery are listed in Table 1. Each of the tasks was scored independently, and an overall score was automatically produced by the software, which has been validated in cases of sudden-onset cognitive impairment (59).

The remaining functional and physiological testing and data collection were carried out face-to-face:

- Functional mobility testing was performed using the 10-meter walk test (10 MWT), which is a well-validated measure that can be completed with relatively low exertion on the part of the participant (60)

Two autonomic measures were completed:

- Root mean square of successive RR interval differences (RMSSD), which is known to correlate with autonomically-mediated changes in heart rate variability (HRV) (61) was collected using mobile app-based photoplethysmography technology developed by Happitech (Happitech, Amsterdam, The Netherlands).
- Postural orthostasis was assessed by monitoring blood pressure and heart rate after three minutes in the supine position and then again after three minutes in the upright position (62) This made use of the guidelines for heart rate changes (≥ 30 beats per minute increase) set out by the American Autonomic Society (63).

Spirometry and peripheral venous oxygen saturation tests were also completed:

- Spirometry with flow volume loop (FVL) and diffusing capacity for carbon monoxide (DLCO) were performed and analyzed following standards approved by the American Thoracic Society and European Respiratory Society (64,65) using the EasyOne Pro® lung function equipment (NDD Medical Technologies; Zurich, Switzerland). Global Lung Function Initiative (GLI) reference values for spirometry and DLCO were employed (66,67)
- Peripheral venous oxygen saturation (SpvO₂) was measured in a sample of venous blood drawn into a heparinized syringe at the time of cannulation of the antecubital vein for apheresis, and again after the procedure. The samples were processed using the GEM Premier 5000 blood gas analyzer (Werfen; Bedford, Maine, USA).

Table 1: Functional testing schedule for a group of patients undergoing H.E.L.P. apheresis.

Measure	Domain	Pre-Apheresis	Post-Apheresis
10-Meter Walk Speed (10 MWT)	Functional Mobility	Yes	Yes
Symptom and Function Checklist	Symptom self-report	Yes	No
Heart Rate Variability (HRV)	Autonomic	Yes	No
Postural orthostasis	Autonomic	Yes	Yes
Spirometry with flow volume loop (FVL)	Respiratory	Yes	Yes
Diffusing Capacity for Carbon Monoxide (DLCO)	Respiratory	Yes	Yes
Peripheral Venous Oxygen Saturation (SpvO ₂)	Respiratory	Yes	Yes
Trails A (Attention)	Cognition	Yes	Yes
Trails B (Mental Flexibility)	Cognition	Yes	Yes
Digital Symbol Substitution (Executive Function)	Cognition	Yes	Yes
Stroop (Executive Function)	Cognition	Yes	Yes
Immediate Recognition (Memory)	Cognition	Yes	Yes
Delayed Recognition (Memory)	Cognition	Yes	Yes

2.3. Microscopic visualization of the blood before and after H.E.L.P. apheresis

Heightened anomalous clotting of fibrin(ogen) and plasma proteins have been formerly observed in Long COVID patients (68-69) using a technique that has previously been described in detail. Naïve platelet-poor plasma (PPP), derived from citrated whole blood (WB) was exposed to the fluorescent dye, Thioflavin T (ThT) (final concentration: 0,005mM) (70), for 30 minutes at room temperature and protected from light. After incubation, 4 µL PPP was smeared on a glass slide and covered with a coverslip. The excitation wavelength for ThT was set to 450–488 nm, while the emission was set to 499–529 nm. The incubated samples were then observed using a Zeiss Axio Observer 7 fluorescent microscope with a Plan-Apochromat 63x/1.4 Oil DIC M27 objective (Carl Zeiss Microscopy, Munich, Germany) (71).

In addition to this assessment of anomalous clotting and plasma proteins, platelet hyperactivation is also assessed in the Long COVID patients using the hematocrit of the citrated blood once the PPP has been removed. This analysis has been previously explained thoroughly. Two fluorescent antibodies are added to the hematocrit: CD62P (staining for platelet surface P-selectin) (68-69) and PAC-1 (staining for activated GP IIb/IIIa) (68-69). During platelet activation, CD62P/P-selectin is released from the platelet cellular granules and relocates to the platelet membrane surface. The PAC-1 antibody detects the neoepitope of activated GP IIb/IIIa receptors. After incubating for 30 minutes at room temperature, 10 μ L hematocrit is placed onto a glass slide and covered with a coverslip. The sample is then viewed using a Zeiss Axio Observer 7 fluorescent microscope with a Plan (71). The excitation wavelength was set at 406–440 nm and the emission at 546–564 nm for the PAC-1 marker. For the CD62P antibody, an excitation of 494–528 nm and an emission wavelength of 618–756 nm was used.

2.4. Blood gas analytics before and after H.E.L.P. apheresis

“Blood gas analysis” is commonly used in our setting as a prognostic tool to evaluate the partial pressures of gas and acid-base content in the blood of patients undergoing H.E.L.P. apheresis. The use of blood gas analysis enables us to understand any related respiratory, circulatory, and metabolic disorders. Blood gas analysis is performed on blood obtained from anywhere in the circulatory system (artery, vein, or capillary). In our setting, venous or arterial was used. An arterial blood gas analysis assesses a patient's partial pressure of oxygen (pO_2) and carbon dioxide (pCO_2). pO_2 provides information on the oxygenation status, whereas pCO_2 offers information on the ventilation status (chronic or acute respiratory failure). Although oxygenation and ventilation can be assessed non-invasively via pulse oximetry and end-tidal carbon dioxide monitoring respectively, arterial blood gas analysis is the standard procedure and was hence performed. While many diseases are evaluated using an arterial blood gas analysis, including acute respiratory distress syndrome (ARDS), severe sepsis, septic shock, hypovolemic shock, diabetic ketoacidosis, renal tubular acidosis, acute respiratory failure, heart failure, cardiac arrest, asthma, and inborn errors of metabolism, we perform this test to assess the endothelial injury relayed as an alteration in blood gases. These alterations are expected in the hypercoagulable state present in Long COVID and post-COVID-19 vaccine syndrome with associated CVS adverse reactions.

2.5. Biomarker analysis in serum before and after H.E.L.P. apheresis

The selection of biomarkers in Long COVID and post-COVID-19 vaccination syndrome is an emerging niche of research. The selection of biomarkers in specific organs affected, as well as biomarkers in COVID-19, Long COVID, and post-COVID-19 vaccination syndrome, focused on endothelial injury, hypercoagulation, platelet hyperactivation and aggregation, and activation of clotting factors. The biomarkers listed in Table 1, both before and after H.E.L.P. apheresis, were anticipated to offer valuable insights into the pathophysiology, prognosis, and treatment outcomes for patients undergoing H.E.L.P. apheresis.

2.6. High-throughput microfluidic imaging of whole blood samples

Real-time deformability cytometry (RT-DC) on WB was performed as described in detail elsewhere (72,73). Briefly, a polydimethylsiloxane (PDMS)-made microfluidic chip with two inlets (sheath- and sample-flow) and an outlet connected by a channel constriction of 20 x 20 μm was mounted onto an inverted microscope (Axiovert-200, Zeiss, Germany) equipped with an LED (CBT-120, Luminus Devices, USA) and a high-speed camera (EoSens CL MC1362, Mikrotron, Germany). Two syringe pumps (NemeSyS, Cetoni, Germany) were used to deliver blood cell suspension and sheath flow through the microfluidic chip at a sample flow rate of 0.015 $\mu\text{L s}^{-1}$ and a sheath flow rate of 0.045 $\mu\text{L s}^{-1}$, resulting in a total flow rate of 0.06 $\mu\text{L s}^{-1}$. The sample consisted of WB and measurement buffer (MB) in a 1 to 20 ratio, respectively. The MB was based on phosphate-buffered saline (PBS, Mg^{2+} -, and Ca^{2+} -free) and 0.6% w/w methylcellulose (4,000 cPs; Sigma Aldrich, USA). Viscosity and osmolarity were adjusted to 26 mPa s at room temperature and 280 – 290 mOsm/kg, respectively. At the end of the channel constriction (the region of interest), an image (250 x 80 pixels) of every cell was captured at a frame rate of 3600 fps using ShapeIn Software (Zellmechanik; Dresden, Germany). In total, 0.45 μL blood was measured. Analysis of microclot-like structures was done using the freeware ShapeOut2 version 2.9.2 (74).

3. Results

3.1. Clinical testing results

A total of 19 patients (six females) completed baseline clinical testing before their first apheresis session. All 19 patients also completed the post-apheresis evaluation 24 hours after treatment. One participant was unable to complete the 10 MWT both pre- and 24 hours post-apheresis due to limitations imposed by their condition.

3.1.1. Cognitive and Functional Outcomes

The results of all pre-and post-apheresis clinical and functional measures are presented in Tables 2-3 and Figure 1. Notably, patients showed significantly improved scores in walking speed measured during the 10 MWT (mean difference: 0.27m/s, $p < 0.001$; Figure 2) and the Digit Symbol Substitution (DSS) cognitive task (mean difference: 13.3, $p < 0.001$) post-apheresis. Post-apheresis improvements in the DSS were significantly correlated with improvements in the 10 MWT ($r = 0.55$, $p < 0.02$). Mean scores on the Trails A, Trails B, Stroop, Immediate Recognition, and Delayed Recognition domains did not show significant changes post-apheresis in comparison to pre-apheresis baseline. However, for the Trails B ($r = -0.68$, $p < 0.002$), Stroop ($r = -0.91$, $p < 0.0001$), and Delayed Recognition ($r = -0.75$, $p < 0.0001$) tests, strong negative correlations were observed between the baseline pre-apheresis score and the change in score post-apheresis, indicating that any post-apheresis improvements in these domains were of greater magnitude in those who scored below average before the procedure.

Table 2: Cognitive function tests before and after H.E.L.P. apheresis.

COGNITIVE DOMAIN	PRE (MEAN \pm SD)	POST (MEAN \pm SD)	P-value
TRAILS A	97.9 \pm 17.1	103.3 \pm 11.4	0.46
TRAILS B	97.4 \pm 15.6	102.2 \pm 11.9	0.23
DIGIT SYMBOL SUBSTITUTION	94.3 \pm 19.6	107.3 \pm 9.5**	0.001
STROOP	88.7 \pm 26.5	100.8 \pm 10.6	0.06
IMMEDIATE RECALL	103.2 \pm 12.1	105.3 \pm 12.8	0.48
DELAYED RECALL	96.8 \pm 18.9	98.1 \pm 14.6	0.78
OVERALL SCORE	98.0 \pm 16.3	105.4 \pm 13.0*	0.03

* $p < 0.05$, ** $p < 0.002$

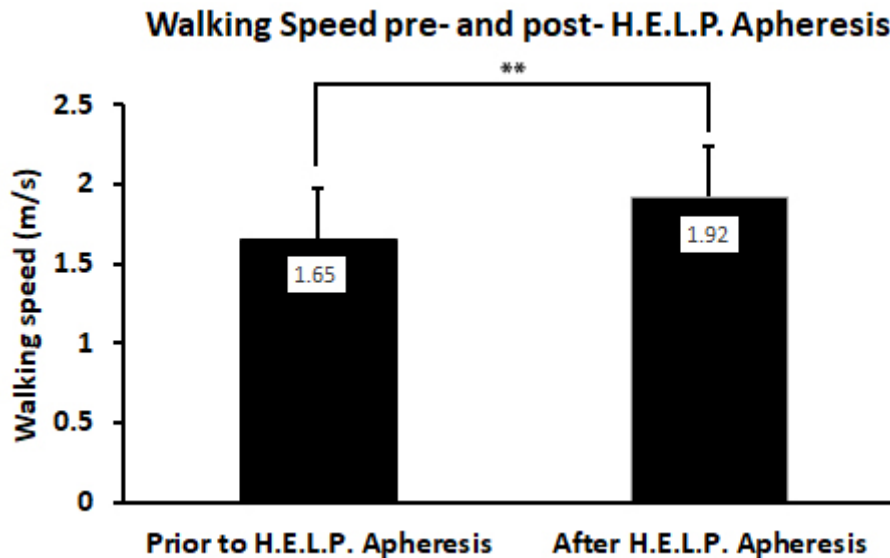


Figure 1: Change in walking speed (meters/second) immediately following one apheresis session compared with baseline. **p<0.001

3.1.2. Autonomic Outcomes

Heart rate variability was only collected at baseline. Patients had an RMSSD that was, on average, 80% lower than the median expected RMSSD for age- and gender-matched controls. Most patients did not show physiological signs consistent with an objective diagnosis of postural orthostatic tachycardia syndrome (POTS), with the average heart rate change after assuming the upright position being 13.2 (\pm 15.0) beats per minute (bpm). Post-apheresis, the average positional heart rate change was 14.2 (\pm 11.0) bpm. However, three patients presented with orthostatic changes that met the AAS criteria for POTS, with an average positional change of 39 (\pm 7.6) bpm; this improved to 14.7 (\pm 9.0) bpm after the H.E.L.P. apheresis procedure. Following apheresis, no patients in the cohort met the AAS criteria for POTS.

3.1.3. Respiratory Outcomes

Mean dynamic lung volumes- both forced expiratory volume in one second (FEV1) and forced vital capacity (FVC)- were normal across the cohort both before and after apheresis. The mean FEV1/FVC ratio (using a cut-off of <70% to define airflow obstruction) ⁷ was unchanged pre- and post-apheresis. Of note, no patient had a significant smoking history (defined as \geq 20 pack-years). Similarly, the mean DLCO expressed as a percentage of the predicted value was normal and remained unchanged after the procedure. Only one patient had a low DLCO of 70% predicted pre-apheresis, and post-apheresis this remained virtually unchanged at 71% predicted. There was no significant difference in mean SpvO₂ measured

before and after apheresis. We elaborate on the interpretation and significance of the SpvO₂ findings in the discussion.

Table 3: Respiratory function tests before and after H.E.L.P. apheresis.

RESPIRATORY DOMAIN	PRE (MEAN ± SD)	POST (MEAN ± SD)	P-value
FEV1	3.7 ± 0.9	3.8 ± 0.8	0.19
FEV1 % Predicted	97.3 ± 13.5	98.8 ± 13.2	0.14
FVC	5.0 ± 1.1	5.0 ± 1.0	0.36
FVC % Predicted	104.6 ± 12.0	105.4 ± 12.0	0.41
FEV1/FVC Ratio	0.8 ± 0.09	0.8 ± 0.08	0.46
DLCO % Predicted	106.9 ± 13.2	106.2 ± 13.8	0.93
SpvO ₂	56.3 ± 19.5	62.0 ± 15.1	0.30

3.2. Microscopic examination of the patient's blood for platelets

Microscopic abnormalities including abnormal platelet aggregation (Fig.2 A3) and spreading (Fig.2 A4) have been noted in Long COVID and post-COVID-19 vaccine syndrome patients in comparison to healthy controls (Fig.2 A1 and A2). Hence, the extent of platelet hyperactivation was assessed before and after H.E.L.P. apheresis. Before H.E.L.P. apheresis the platelets were seen in a hyperactivated phase (Fig.2 B1 and B2) with pseudopodia formation and enhanced aggregation and spreading. Following H.E.L.P. apheresis, the normal platelet morphology is regained (Fig.2 B3 and B4).

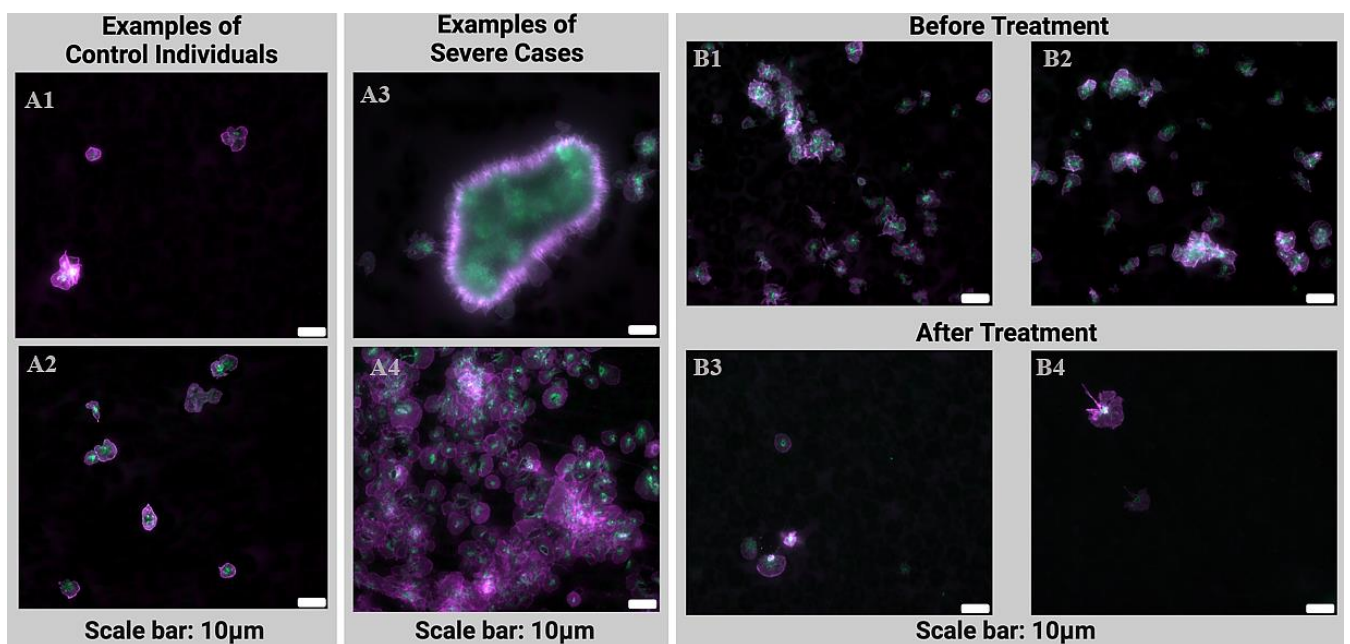


Figure 2: Illustration of platelet hyperactivation, spreading, and clumping in Long COVID, and how this hyperactivation is reduced with H.E.L.P. apheresis and anticoagulant therapy. A1-A2. Examples of minimal platelet hyperactivation in healthy individuals. In control patients, minimal platelet spreading, and aggregation is observed. A3-A4. Example micrograph images from severe Long COVID cases. Image A3 demonstrates severe platelet aggregation (diameter $\pm 80\mu\text{M}$), while Image A4 illustrates an increased concentration and spreading of hyperactivated platelets. B1-B2. Micrograph images are taken of a patient before treatment with H.E.L.P. apheresis. Although the platelet aggregation is not severe in this patient, the concentration of hyperactivated platelets is significantly noticeable. B3-B4. Micrograph images were taken after the patient's treatment with H.E.L.P. apheresis. The concentration of hyperactivated platelets was greatly reduced, along with reduced aggregating structures.

3.3. Amyloid-like micro clot structures, endothelial damage, plasma protein misfolding, and fibrinogen-like structures in Long COVID and post-COVID-19 vaccine syndrome

Additionally, patients with Long COVID and post-COVID-19 vaccination syndrome display a consistent presence of amyloid-like microclot structures, endothelial damage, plasma protein misfolding, and fibrinogen-like structures, which are hypothesized to promote ischemia and cause vessel obstruction or thickening. In control patients, minimal amyloid-like microclots, plasma protein misfolding, and endothelial damage are observed (Fig.3 A1 and A2).

However, in Long COVID and post-COVID-19 vaccination syndrome patients, elongated structures are observed (Fig.3 A3) that are thought to contain misfolded fibrinogen and small microclot structures. With H.E.L.P. apheresis, this presence of endothelial damage and misfolded plasma proteins (Fig.3 B1 and B2) is minimized, and the microscopic examination reveals a decreased presence of these structures (Fig.3 B3 and B4).

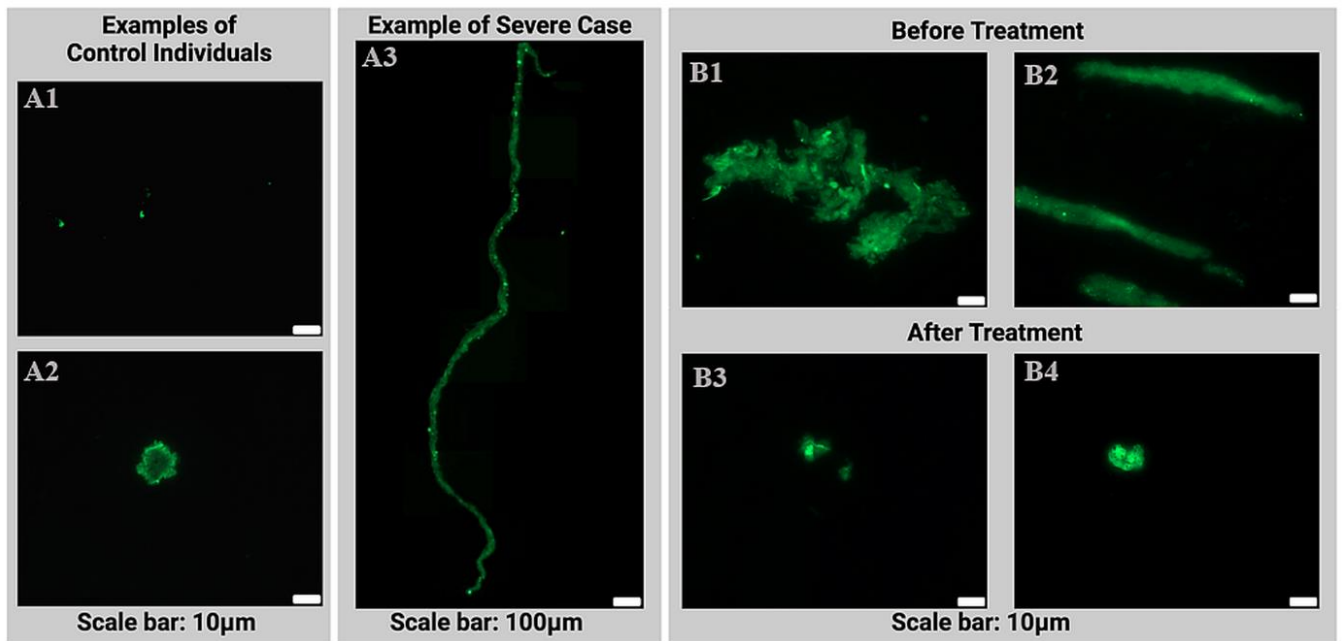


Figure 3. Illustration of amyloid-like microclot structures, endothelial damage, plasma protein misfolding, and fibrinogen-like structures in Long COVID, and how this presence is reduced with H.E.L.P. apheresis and anticoagulant therapy. A1-A2. Examples of amyloid-like microclot structures, endothelial damage, and plasma protein misfolding in healthy individuals. In control patients, minimal presence is observed. A3. Example micrograph image from a severe Long COVID case. Image A3 demonstrates a worm-like structure, which is hypothesized to contain misfolded fibrinogen and small microclot-like structures. The length of the structure is around 2400 μM (2,4 mm). B1-B2. Micrograph images are taken of a patient before treatment with H.E.L.P. apheresis. A significant presence of endothelial damage and amyloid-like microclot structures is observed. B3-B4. Micrograph images were taken after the patient's treatment with H.E.L.P. apheresis. The concentration of these structures was greatly reduced.

3.4. Long COVID and post-COVID-19 vaccination syndrome patients exhibited blood gas derangements characterized by low oxygen (pO_2) levels and elevated carbon dioxide (pCO_2) levels in both arterial and venous blood

A key method for evaluating the effectiveness of H.E.L.P. apheresis was through the comparison of blood pO_2 , pCO_2 , and pH values in patients before and after the procedure. A remarkable increase in pO_2 and a noticeable decline in pCO_2 was observed in our patient groups. Additionally, the normalization of the pH values indicated the impact of H.E.L.P. apheresis on addressing metabolic acidosis. Figure 3 illustrating this in a large cohort of patients can be seen below, while additional data can be seen in the supplementary material.

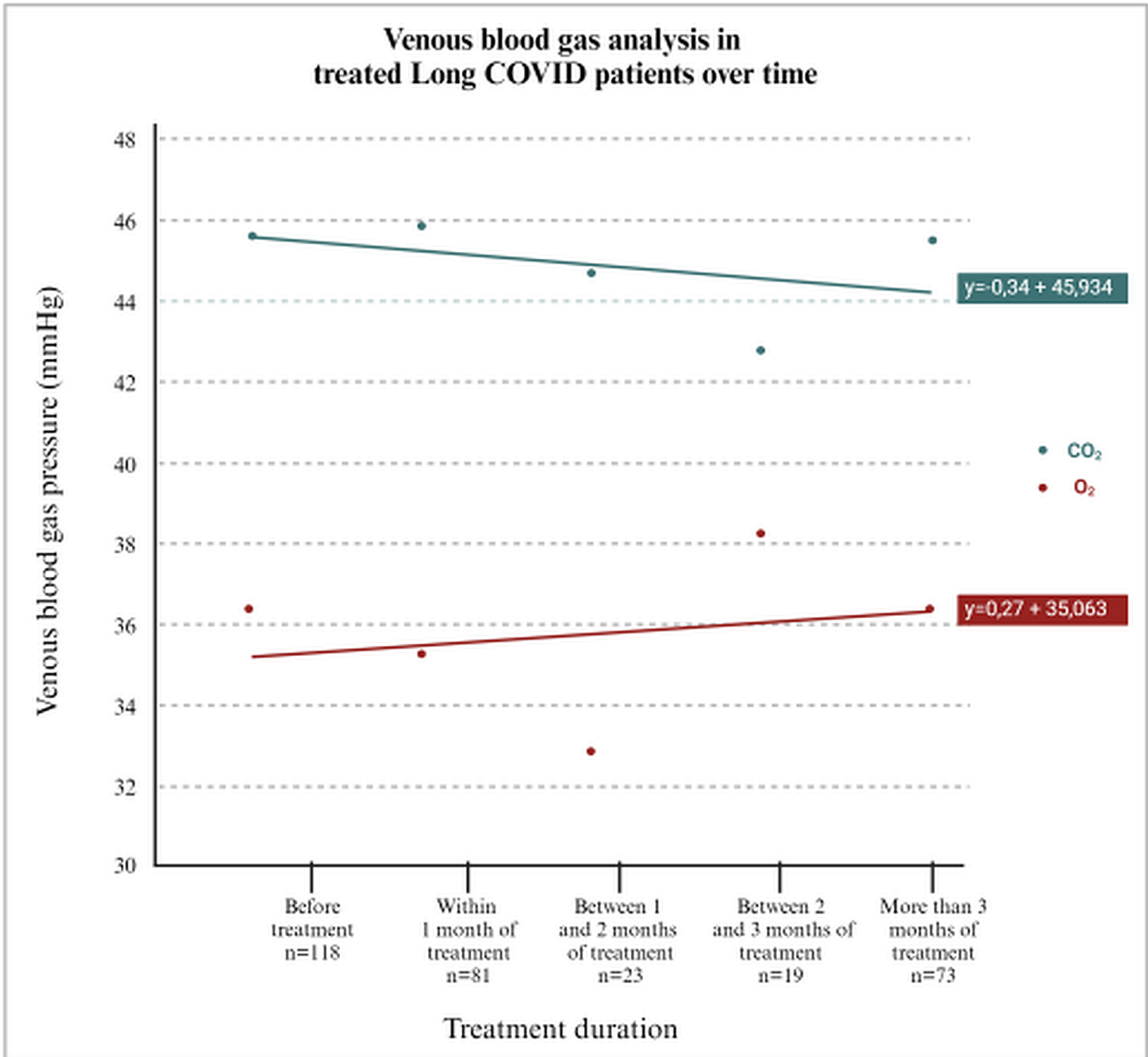


Figure 4. Blood gas analyses over time (X-axis) in Long COVID, post-COVID-19-vaccination syndrome, or “combination” patients (n) treated with H.E.L.P. apheresis and anticoagulants. The Y-axis is reflective of average pCO₂ (mmHg) which decreases over time with treatment with a linear regression of $m=-0,97$, while the average pO₂ (mmHg) was seen to increase with a linear regression of $m=1,158$. Examples of individual patient's blood gas pressure can be found in the supplementary material.

3.5. Serum biomarker derangements seen in Long COVID and post-COVID-19 vaccination syndrome and how these biomarkers improve with H.E.L.P. apheresis.

Typical indicators of hypercoagulation and systemic inflammation, such as C-reactive protein (CRP), D-Dimer, bleeding time, clotting time, and partial prothrombin time (aPTT), did not show any trends with H.E.L.P. apheresis treatment, and varied patient to patient. However, one interesting marker that was found to be altered in cases of Long COVID and post-COVID-19 vaccination syndrome is elevated IgG against the nucleocapsid (N) antigen in Long COVID patients. This phenomenon was not observed in post-COVID-19 vaccination syndrome patients. Additionally, a reduction of spike protein levels was observed in several patients after treatment with H.E.L.P. apheresis (Figure 5), with a 92% reduction.

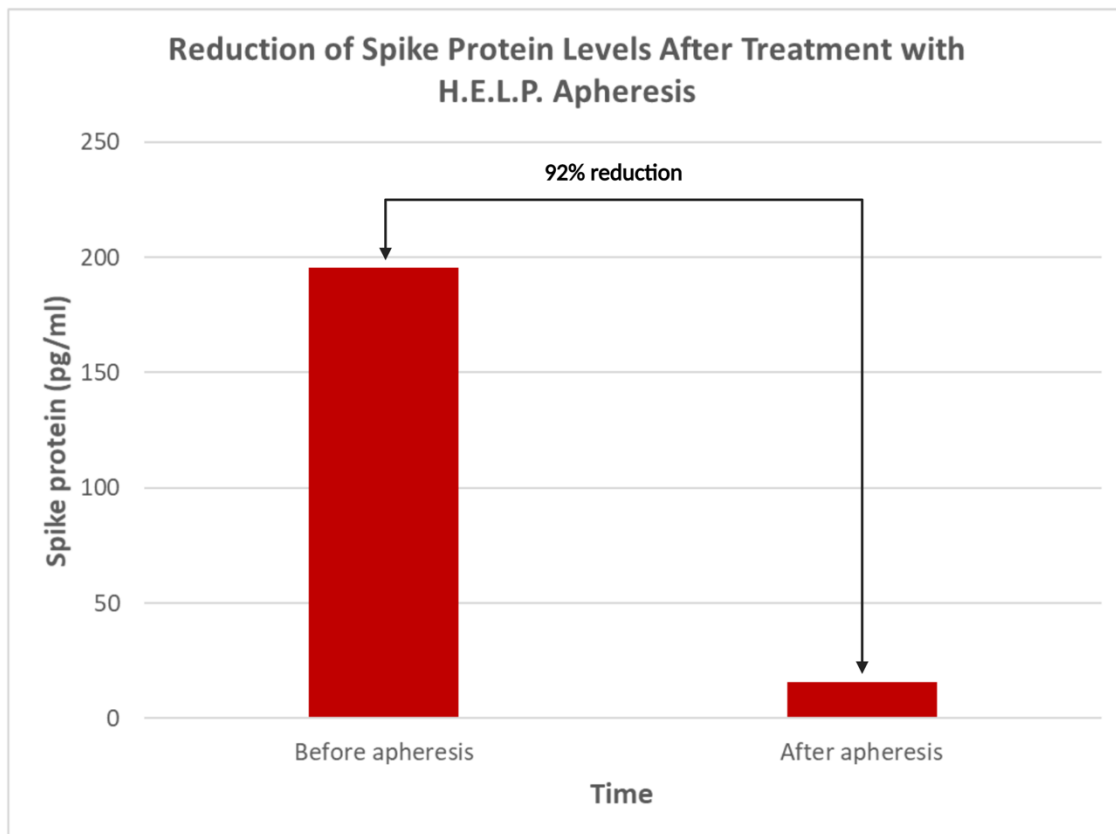


Figure 5. Reduction of spike protein levels (pg/ml) after treatment with H.E.L.P. apheresis. A 92% reduction of the spike protein was observed.

3.6. High-throughput microfluidic imaging of whole blood samples

Real-time deformability cytometry was used to assess microclot-like structures in WB of Long COVID patients before and after H.E.L.P. apheresis. RT-DC is a microfluidic-based imaging technology used to acquire the physical properties of particles in flow at a speed of up to 1000 events per second and has been used previously to document changes in the physical phenotypes

of blood cells during acute COVID-19 infection (75). We used a simple gating strategy to identify microclot-like structures by plotting 100,000 of the approximately 1.2 million acquired events for each patient, according to their projected area and deformation. We then applied a polygon gate to detect events as shown in Figure 6A. Representative appearances of gated microclot-like structures are illustrated in Figure 6B, whilst Table 4 displays the overall analysis of the microclot-like structures. A significant reduction in the overall count of microclot-like structures and a reduction in the percentage of microclot-like structures to all measured events in a blood sample was noted immediately after apheresis ($p < 0.05$; Figures 6A and 6B). The clot size (projected area) and the standard deviation of the projected area did not change (Figures 6C and 6D). However, it should be kept in mind that not all events are necessarily clots, as damaged endothelial cells or cellular debris generated by the apheresis process may have been present and therefore recognized in the analysis.

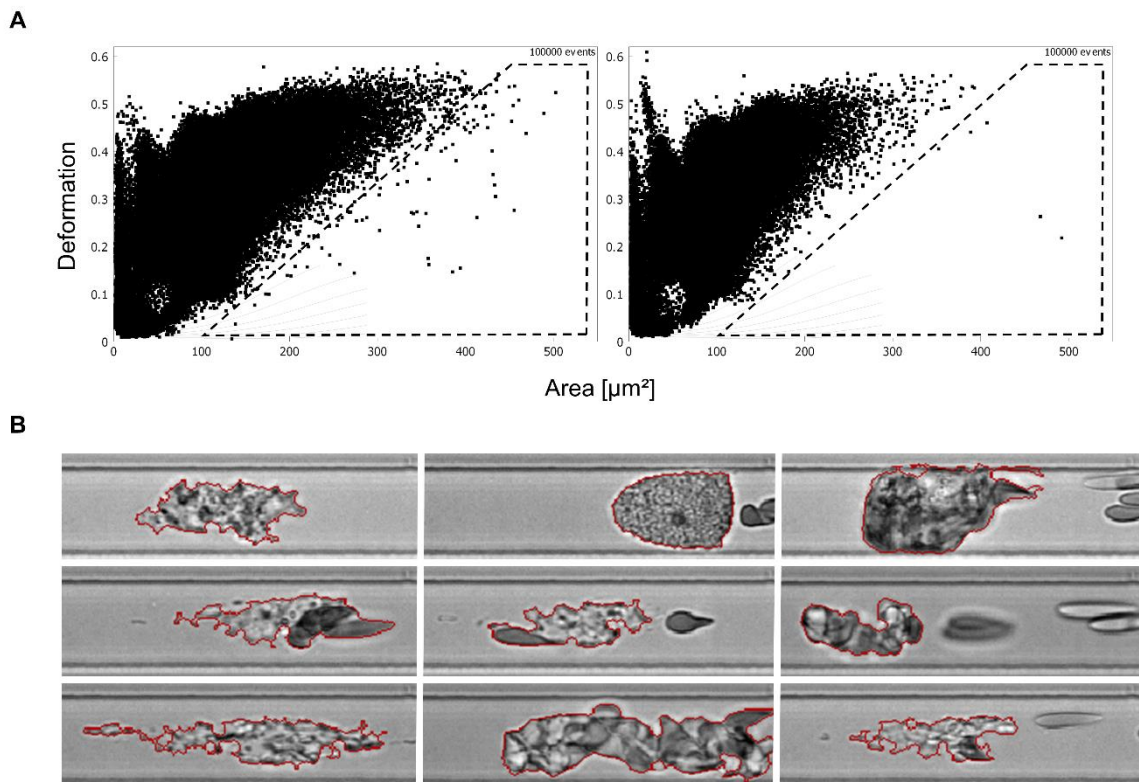


Figure 6. Representative RT-DC measurements of whole blood (approximately 1.2 million event images per participant were acquired). **A.** Gating strategy to identify microclot-like structures from WB before and directly after H.E.L.P. apheresis. Scatter plots of area and deformation show representative RT-DC measurements. Every dot is a measured event ranging from normal blood cells or cell agglomerates to microclot-like structures (100,000 events are shown). The events outside the gate (dashed polygon) are blood cells or cell agglomerates. **B.** Representative images of microclot-like structures in RT-DC measurement channel. Red lines outline the event contour, which automatically gets assigned to the event in real-time and is the basis for size analysis (area within the contour in μm^2).

Table 4. Overall analysis of n=16 patients of microclot-like structures derived from RT-DC measurements. **A.** count of microclot-like structures per 0.45 μl of blood, **B.** microclot-like structures expressed as a percentage of all measured events (blood cells and cell agglomerates), **C.** projected area (μm^2) of microclot-like structures; and **D.** standard deviation of the projected area (μm^2) of microclot-like structures before and directly after H.E.L.P. apheresis.

	Measurement	Before apheresis (Mean \pm SEM)	Directly after apheresis (Mean \pm SEM)	P-value
A	Count [per 0.45 μl]	13 \pm 1.9	7.86 \pm 1.44	0.0136
B	% [of all events]	0.00081 \pm 0.00015	0.00053 \pm 0.0001	0.0769
C	Area [μm^2]	420.1 \pm 24.8	385.4 \pm 15.6	0.2514
D	Area std [μm^2]	129.7 \pm 9.6	104.3 \pm 11.4	0.0101

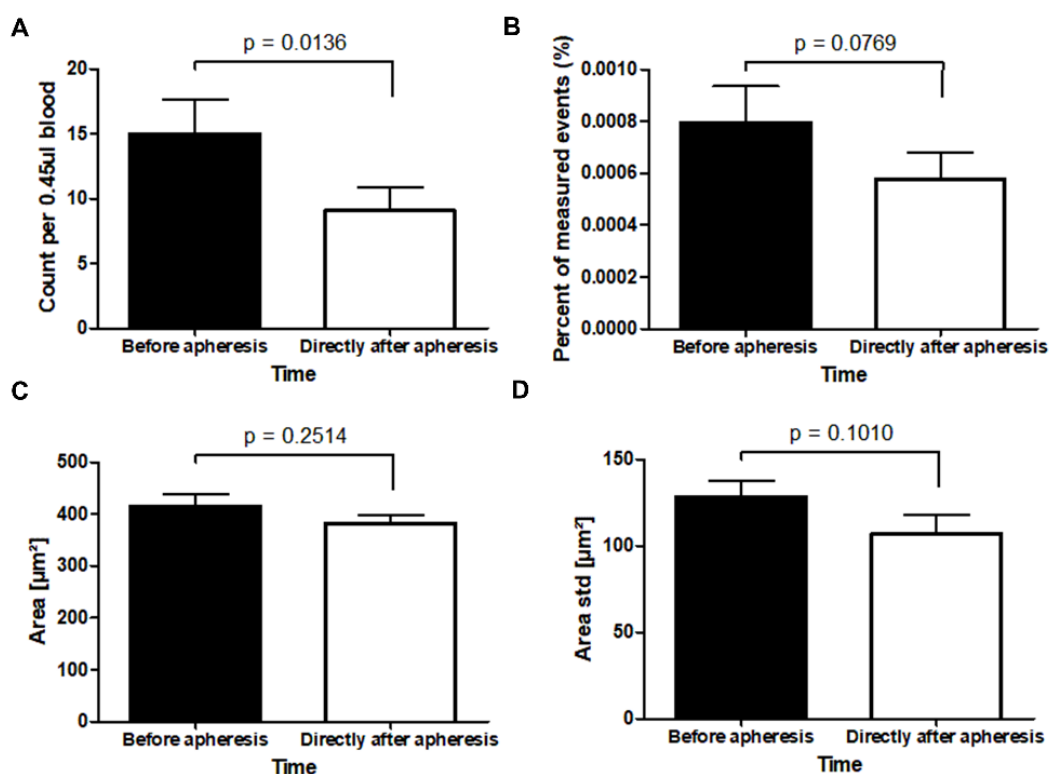


Figure 7. Analysis of microclot-like structures from RT-DC measurements of 0.45 μl of whole blood. **A-D.** Bar plots of n = 16 patients (repeat samples were not received for three patients). **A.** Count of microclot-like structures per 0.45 μl of blood. **B.** Microclot-like structures expressed as a percentage of all measured events (blood cells and cell agglomerates). **C.** Projected area (μm^2) of microclot-like structures. **D.** Standard deviation of the projected area (μm^2) of microclot-like structures.

4. Discussion

This paper debates and provides comprehensive evidence of the benefits of H.E.L.P. apheresis in a group of patients with Long COVID and post-COVID-19 vaccination syndrome. Essential to the understanding of these conditions is the fact that patients present with multiorgan and multisystem dysfunction that is difficult to ascribe to a single pathogenetic event. Therefore, the broad positive impacts of H.E.L.P. apheresis position it as an ideal therapeutic approach. Firstly, circulating cytokines, CRP, harmful lipids, and fibrinogen are reduced considerably up to 50% within 2 hours. As a result, the flow and deformation of the pulmonary microcirculation have been seen to be immediately relieved—without reduction of the erythrocyte concentration. Fibrinogen is the effector of plasmatic coagulation and a decisive determinant in vascular microcirculation, viscosity of the blood, and erythrocyte aggregability. Owing to the use of unfractionated heparin in H.E.L.P. apheresis, the antithrombotic effect is maximal. Additionally, in-depth initial studies investigating the influence of H.E.L.P. apheresis on the kinetics of the procoagulation and fibrinolytic cascades have shown that, except for antithrombin III (which is reduced by 25%), the precursors of both procoagulation and fibrinolytic cascades are reduced by 35–50% within 2 hours. As a result, H.E.L.P. apheresis de-escalates the excessive coagulation without any risk of bleeding owing to the complete adsorption of unfractionated heparin. In the case of COVID-19, H.E.L.P. apheresis is also advantageous owing to its ability to diminish the trigger of the overwhelming immune response: the SARS-CoV-2 S protein. The S protein can induce deleterious effects on the endothelium and the clotting cascade, resulting in ischemia and a decline in organ function and performance. Even if ischemia is not an aetiological cause, H.E.L.P. apheresis (and other drugs) offers improvements in decreasing the extent of endothelial injury and hypercoagulation in patients, as well as improving symptoms.

This improvement is visualized using fluorescent microscopy analysis. Before H.E.L.P. apheresis treatment, many of the patients displayed derangements in platelet morphology and abnormal fibrinogen-like strands, coupled with endothelial dysfunction and the presence of amyloid-like microclots. The notable improvements depicted following H.E.L.P. apheresis are remarkable and correlate with an enhanced clinical presentation. This shows evidence of the benefits of H.E.L.P. apheresis in Long COVID and post-COVID-19 vaccination syndrome patients. The second most significant criterion to assess the benefits of H.E.L.P. apheresis is

the blood gas parameters in the form of pO₂ and pCO₂ in arterial and venous blood samples collected before and after H.E.L.P. apheresis treatments. The elevation in pO₂ and reduction in pCO₂ are evidence of improved microcirculation and oxygen exchange. Measured biomarker levels of individual organs and endothelial were also used to assess the benefits of H.E.L.P. apheresis in Long COVID and post-COVID-19 vaccination syndrome patients. Our results show that with and without supplementary anticoagulant medication, H.E.L.P. apheresis helped reduce the biomarker levels of organ damage to near baseline levels. While the investigations conducted before and after H.E.L.P. apheresis treatment suggest theoretical improvements, the pivotal criterion for assessing the impact of H.E.L.P. apheresis is the evaluation of symptoms during the treatment. Our study shows a clear improvement in patient symptoms after the procedure, and when combined with anticoagulant medication to further combat the hypercoagulability state of the patient. We show that, after H.E.L.P. apheresis treatment, organ perfusion in general improves significantly in the affected individuals undergoing the procedure (Table 3). A hypothesis suggests that the patients who did not experience significant benefits may fall into two categories: those with reduced compliance and those with notable non-COVID-19-related comorbidities. It is important to mention here that the choice of the patients to undergo H.E.L.P. apheresis in our setting depended on numerous factors; including the extent of platelet hyperactivation, the presence of fibrinogen-like strands and damaged endothelium, deranged biomarkers, and the clinical severity of the patients. Patients classified as “mild” were advised to take a triple anticoagulant therapy to observe improvements.

We have previously reported on the mechanism through which H.E.L.P. apheresis reduces organ damage in COVID-19 and Long COVID. However, a novel aspect of the current study is the documentation of its benefits in post-COVID-19 vaccination syndrome. This syndrome has been on the rise since the latter part of 2022 and early 2023. In addition to the known mechanisms by which heparin helps in prothrombotic states, we are also studying the possibility of the binding effects of heparin to the receptor binding domain (RBD) of the spike protein, and adsorption of conotoxins harboring gut microbes released by SARS-CoV-2. These mechanisms appear to be additional pathways that H.E.L.P. apheresis may benefit both Long COVID and post-COVID-19 vaccination syndrome patients. It is also important to mention that H.E.L.P. apheresis is not restricted to a two- or three-hour treatment modality. The system can be recirculated for many hours until the precipitate filter is saturated. As the

precipitate filter can also be renewed and replaced during the procedure, the fibrinogen concentration theoretically could be reduced considerably if desired.

Since the patients improved clinically with low-dose heparin post-H.E.L.P. apheresis and an improvement in the fluorescent microscopy results and biomarkers was noted, this therapy may be beneficial in patients with Long COVID and those with post-COVID-19 vaccination syndrome. As a sustained production of S protein has been shown to increase hypercoagulability in these patients, H.E.L.P. apheresis is emerging as a methodology of choice with its ability to combat endothelial injury, antithrombotic effects, and dysregulated cytokine production.

5. Conclusion and Future Directions

To treat COVID-19 most effectively, Long COVID, and post-COVID-19 vaccination syndrome, it is essential to identify the underlying factors that trigger symptom presentation in these patients. It appears that the S protein incites vascular events responsible for an array of vascular and flow dynamics that result in tissue ischemia and injury. Autoimmune antibodies formed in patients with Long COVID additionally exacerbate the previously injured vascular endothelium and complicate the clinical picture. H.E.L.P. apheresis, combined with anticoagulant medication targeting the coagulation cascade, has proven to be enormously beneficial in the included patients. This calls for future research to identify currently unknown pathways, aiding patients with COVID-19, Long COVID-19, post-COVID-19, and vaccination syndrome. Securing funding and bringing these conditions to light is essential to ensure the affordability and accessibility of these treatments. This is crucial to realizing the widespread benefits of H.E.L.P. apheresis for the growing number of patients affected by COVID-19, Long COVID-19, and post-COVID-19 vaccination syndrome.

References

1. Otifi HM, Adiga BK. Endothelial Dysfunction in Covid-19 Infection. *Am J Med Sci*. 2022 Apr;363(4):281-287. doi: 10.1016/j.amjms.2021.12.010. Epub 2022 Jan 31. PMID: 35093394; PMCID: PMC8802031.
2. Xu SW, Ilyas I, Weng JP. Endothelial dysfunction in COVID-19: an overview of evidence, biomarkers, mechanisms and potential therapies. *Acta Pharmacol Sin*. 2023 Apr;44(4):695-709. doi: 10.1038/s41401-022-00998-0. Epub 2022 Oct 17. PMID: 36253560; PMCID: PMC9574180.
3. Hoffmann M, Kleine-Weber H, Schroeder S, Krüger N, Herrler T, Erichsen S, Schiergens TS, Herrler G, Wu NH, Nitsche A, Müller MA, Drosten C, Pöhlmann S. SARS-CoV-2 Cell Entry Depends on ACE2 and TMPRSS2 and Is Blocked by a Clinically Proven Protease Inhibitor. *Cell*. 2020 Apr 16;181(2):271-280.e8. doi: 10.1016/j.cell.2020.02.052. Epub 2020 Mar 5. PMID: 32142651; PMCID: PMC7102627.
4. Li W., Moore M.J., Vasilieva N., Sui J., Wong S.K., Berne M.A., Somasundaran M., Sullivan J.L., Luzuriaga K., Greenough T.C. Angiotensin-converting enzyme 2 is a functional receptor for the SARS coronavirus. *Nature*.
5. Glowacka I., Bertram S., Müller M.A., Allen P., Soilleux E., Pfefferle S., Steffen I., Tsegaye T.S., He Y., Gnirss K. Evidence that TMPRSS2 activates the severe acute respiratory syndrome coronavirus spike protein for membrane fusion and reduces viral control by the humoral immune response. *J. Virol*.
6. Zhou P, Yang XL, Wang XG, Hu B, Zhang L, Zhang W, et al. A pneumonia outbreak associated with a new coronavirus of probable bat origin. *Nature*. (2020) 579:270–3. doi: 10.1038/s41586-020-2012-7
7. Zhang H, Zhou P, Wei Y, Yue H, Wang Y, Hu M, et al. Histopathologic changes and SARS-CoV-2 immunostaining in the lung of a patient with COVID-19. *Ann Intern Med*. (2020) 172:629–632. doi: 10.7326/L20-0895
8. *Epidemiologisches Bulletin* 14/2020. Schwereinschätzung von COVID-19 mit Vergleichsdaten zu Pneumonien aus dem Krankenhaussentinel für schwere akute Atemwegserkrankungen am RKI (ICOSARI) [Severity assessment of COVID-19 with comparative data on pneumonia from the hospital sentinel for severe acute respiratory diseases at the RKI (ICOSARI)]. (2020).
9. Bhatraju PK, Ghassemieh BJ, Nichols M, Kim R, Jerome KR, Nalla AK, et al. Covid-19 in critically ill patients in the seattle region—case series. *NEJM*. (2020) 382:2012–2022. doi: 10.1056/NEJMoa2004500
10. Baig AM, Khaleeq A, Ali U, Syeda H. Evidence of the COVID-19 Virus Targeting the CNS: Tissue Distribution, Host-Virus Interaction, and Proposed Neurotropic Mechanisms. *ACS Chem Neurosci*. 2020 Apr 1;11(7):995-998. doi: 10.1021/acchemneuro.0c00122. Epub 2020 Mar 13. PMID: 32167747.

11. Madjid M, Safavi-Naeini P, Solomon SD, Vardeny O. Potential effects of coronaviruses on the cardiovascular system: a review. *JAMA Cardiol.* (2020)5:831–40. doi: 10.1001/jamacardio.2020.1286
12. Guo T, Fan Y, Chen M, Wu X, Zhang L, He T, et al. Cardiovascular implications of fatal outcomes of patients with coronavirus disease 2019 (COVID-19). *JAMA Cardiol.* (2019) 5:811–8. doi: 10.1001/jamacardio.2020.1017
13. Inciardi RM, Lupi L, Zaccone G, Italia L, Raffo M, Tomasoni D, et al. Cardiac involvement in a patient with coronavirus disease 2019 (COVID-19). *JAMA Cardiol.* (2020) 5:819–24. doi: 10.1001/jamacardio.2020.1096
14. Yang C, Jin Z. An acute respiratory infection runs into the most common noncommunicable epidemic-COVID-19 and cardiovascular diseases. *JAMA Cardiol.* (2020) 5:743–4. doi: 10.1001/jamacardio.2020.0934
15. Parra-Medina R, Herrera S, Mejia J. Systematic review of microthrombi in COVID-19 autopsies. *Acta Haematol.* (2021) 144:476–83. doi: 10.1159/000515104
16. Caputo I, Caroccia B, Frasson I, Poggio E, Zamberlan S, Morpurgo M, et al. Angiotensin II promotes SARS-CoV-2 infection via upregulation of ACE2 in human bronchial cells. *Int J Mol Sci.* (2022) 23:5125. doi: 10.3390/ijms23095125
17. Jackson CB, Farzan M, Chen B, Choe H. Mechanisms of SARS-CoV-2 entry into cells. *Nat Rev Mol Cell Biol.* 2022;23:3-20. doi: 10.1038/s41580-021-00418-x
18. Varga Z, Flammer AJ, Steiger P, Haberecker M, Andermatt R, Zinkernagel AS, et al. Endothelial cell infection and endothelitis in COVID-19. *Lancet.* (2020) 395:1417–1418. doi: 10.1016/S0140-6736(20)30937-5
19. Viles-Gonzalez JF, Fuster V, Badimon JJ. Links between inflammation and thrombogenicity in atherosclerosis. *Curr Mol Med.* (2006) 6:489–99. doi: 10.2174/156652406778018707
20. Morel O, Kessler L, Ohlmann P, Bareiss P. Diabetes and the platelet: toward new therapeutic paradigms for diabetic atherothrombosis. *Atherosclerosis.* (2010) 212:367–76. doi: 10.1016/j.atherosclerosis.2010.03.019
21. Chiva-Blanch G, Peña E, Cubedo J, García-Arguinzonis M, Pané A, Gil PA, et al. Molecular mapping of platelet hyperreactivity in diabetes: the stress proteins complex HSPA8/Hsp90/CSK2a and platelet aggregation in diabetic and normal platelets. *Transl Res.* (2021) 235:1–14. doi: 10.1016/j.trsl.2021.04.003
22. Ye Q, Wang B, Mao J. The pathogenesis and treatment of the ‘Cytokine Storm’ in COVID-19. *J. Infect.* (2020) 80:607–13. doi: 10.1016/j.jinf.2020.03.037

23. Mycroft-West C, Su D, Elli S, Guimond S, Miller G, Turnbull J, et al. The 2019 coronavirus (SARS-CoV-2) surface protein (Spike) S1 receptor binding domain undergoes conformational change upon heparin binding. *BioRxiv*. (2020). doi: 10.1101/2020.02.29.971093
24. Araos J, Alegría L, García P, Damiani F, Tapia P, Soto D, et al. Extracorporeal membrane oxygenation improves survival in a novel 24-hour pig model of severe acute respiratory distress syndrome. *Am J Transl Res*. (2016) 8:2826–37.
25. Neto AS, Schmidt M, Azevedo LCP, Bein T, Brochard L, Beutel G, et al. Associations between ventilator settings during extracorporeal membrane oxygenation for refractory hypoxemia and outcome in patients with acute respiratory distress syndrome: a pooled individual patient data analysis. *Intensive Care Med*. (2016) 42:1672–84. doi: 10.1007/s00134-016-4507-0
26. Helmerhorst HJ, Schultz MJ, van der Voort PH, de Jonge E, van Westerloo DJ. Bench-to-bedside review: the effects of hyperoxia during critical illness. *Crit Care*. (2015) 19:284. doi: 10.1186/s13054-015-0996-4
27. Helmerhorst HJ, Roos-Blom MJ, van Westerloo DJ, de Jonge E. Association between arterial hyperoxia and outcome in subsets of critical illness: a systematic review, meta-analysis, and meta-regression of cohort studies. *Crit Care Med*. (2015) 43:1508–19. doi: 10.1097/CCM.0000000000000998
28. Seidel D, Armstrong VW, Schuff-Werner P, Eisenhauer T. Removal of low-density lipoproteins (LDL) and fibrinogen by precipitation with heparin at low pH: clinical application and experience. *J Clin Apheresis*. (1988) 4:78–81. doi: 10.1002/jca.2920040207
29. Seidel D, Armstrong VW, Schuff-Werner P. The HELP-LDL-Apheresis multicentre study, an angiographically assessed trial on the role of LDL-apheresis in the secondary prevention of coronary heart disease. I evaluation of safety and cholesterol-lowering effects during the first 12 months. *Eur J Clin Inv*. (1991) 21:375–83. doi: 10.1111/j.1365-2362.1991.tb01384.x
30. Jaeger BR, Arron HE, Kalka-Moll WM, Seidel D. The potential of heparin-induced extracorporeal LDL/fibrinogen precipitation (H.E.L.P.)-apheresis for patients with severe acute or chronic COVID-19. *Front Cardiovasc Med*. 2022;9:1007636. doi: 10.3389/fcvm.2022.1007636
31. Jaeger BR, Tsobanelis T, Bengel F, Schwaiger M, Seidel D. Long-term prevention of premature coronary atherosclerosis in homozygous familial hypercholesterolemia. *J Pediatrics*. (2002) 141:125–8. doi: 10.1067/mpd.2002.124384
32. Eisenhauer T, Armstrong VW, Wieland H, Fuchs C, Nebendahl K, Scheler F, et al. Selective continuous elimination of low density lipoproteins (LDL) by heparin precipitation: first clinical application. *Trans Am Soc Artif Organs*. (1986) 32:104–7.

33. Schuff-Werner P, Gohlke H, Bartmann U, Baggio G, Corti MC, Dinsenbacher A, et al. The HELP-LDL-apheresis multicentre study, an angiographically assessed trial on the role of LDL-apheresis in the secondary prevention of coronary heart disease. II Final evaluation of the effect of regular treatment on LDL-cholesterol plasma concentrations and the Course of CoronaryHeartDisease. *Eur J Clin Invest.* (1994) 24:724–32. doi: 10.1111/j.1365-2362.1994.tb01068.x
34. Thiery J, Walli AK, Janning G, Seidel D. Low-density lipoprotein plasmapheresis with and without lovastatin in the treatment of the homozygous form of familial hypercholesterolaemia. *Eur J Pediatr.* (1990)149:716–21. doi: 10.1007/BF01959530
35. Mellwig KP, Schmidt HK, Brettschneider-Meyer A, Meyer H, Jaeger BR, Walli AK, et al. Coronary heart disease in childhood in familial hypercholesteremia. Maximum therapy with LDL apheresis. *Internist.* (2003)44:476–80. 10.1007/s00108-002-0832-1
36. Schuff-Werner P. Clinical Long-Term Results of H.E.L.P.-Apheresis. *Z Kardiol.* (2003) 92: III 28–9.
37. Jaeger BR, Richter Y, Nagel D, Heigl F, Vogt A, Roeseler E, et al. Longitudinal cohort study on the effectiveness of lipid apheresis treatment to reduce high lipoprotein (a) levels and prevent major adverse coronary events. *Nat Clin Pract Cardiovasc Med.* (2009) 6:229–39. doi: 10.1038/ncpcardio1456
38. Jaeger BR, Bengel FM, Odaka K, Uberfuhr P, Labarrere CA, Bengsch S, et al. Changes in myocardial vasoreactivity after drastic reduction of plasma fibrinogen and cholesterol: a clinical study in long-term heart transplant survivors using positron emission tomography. *J Heart Lung Transplant.* (2005) 24:2022–30. doi: 10.1016/j.healun.2005.05.009
39. Park JW, Merz M, Braun P. Regression of transplant coronary artery disease during low-density lipoprotein apheresis. *JHLT.* (1997) 16:290–97.
40. Jaeger BR, Meiser B, Nagel D, Uberfuhr P, Thiery J, Brandl U, et al. Aggressive lowering of fibrinogen and cholesterol in the prevention of graft vessel disease after heart transplantation. *Circulation.* (1997) 96: II 154–8
41. Jaeger BR, Braun P, Nagel D, Park JW, Gysan DB, Oberhoffer M, et al. A combined treatment of statins and HELP apheresis for treatment of cardiac allograft vasculopathy. *Atherosclerosis Suppl.* (2002) 141:331–6.
42. Labarrere CA, Woods JR, Hardin JW, Campana GL, Ortiz MA, Jaeger BR, et al. Early Prediction of cardiac allograft vasculopathy and heart transplant failure. *Am J Transplant.* (2011) 11:528–35. doi: 10.1111/j.1600-6143.2010.03401.x
43. Labarrere CA, Woods JR, Hardin JW, Jaeger BR, Zembala M, Deng MC, et al. Early inflammatory markers are independent predictors of cardiac allograft vasculopathy in heart-transplant recipients. *PLoS ONE.* (2014) 9:e113260. doi: 10.1371/journal.pone.0113260
44. Labarrere CA, Jaeger BR, Kassab GS. Cardiac allograft vasculopathy: microvascular arteriolar capillaries (“Capioles”) and survival. *Front Biosc.* (2017) 9:110–28. doi: 10.2741/e790

45. Oberhoffer M, Eifert S, Jaeger B, Blessing F, Beiras-Fernandez A, Seidel D, et al. Postoperative heparin-mediated extracorporeal low-density lipoprotein fibrinogen precipitation aphaeresis prevents early graft occlusion after coronary artery bypass grafting. *Surg J.* (2016) 2:e5–9. doi: 10.1055/s-0036-1584167
46. Wang Y, Walli AK, Schulze A, Blessing F, Fraunberger P, Thaler C, et al. Heparin-mediated extracorporeal low density lipoprotein precipitation as a possible therapeutic approach in preeclampsia. *Transfus Apheres Sci.* (2006) 35:103–10. doi: 10.1016/j.transci.2006.05.010
47. Contini C, Pütz G, Pecks U, Winkler K. Apheresis as emerging treatment option in severe early onset preeclampsia. *Atheroscler Suppl.* (2019) 40:61–7. doi: 10.1016/j.atherosclerosissup.2019.08.028
48. Walzl M, Lechner H, Walzl B, Schied G. Improved neurological recovery of cerebral infarctions after plasmapheretic reduction of lipids and fibrinogen. *Stroke.* (1993) 24:1447–51. doi: 10.1161/01.STR.24.10.1447
49. Walzl B, Walzl M, Valetitsch H, Lechner H. Increased cerebral perfusion following reduction of fibrinogen and lipid fractions. *Haemostasis.* (1995) 25:137–43. doi: 10.1159/000217153
50. Jaeger BR. The HELP System for the treatment of atherothrombotic disorders: a review. *Therap Apheres Dialy.* (2003) 7:391–6. doi: 10.1046/j.1526-0968.2003.00072.x
51. Jaeger BR, Kreuzer E, Knez A, Leber A, Uberfuhr P, Börner M, et al. Case reports on emergency treatment of cardiovascular syndromes through heparinmediated low-density lipoprotein/fibrinogen precipitation: a new approach to augment cerebral and myocardial salvage. *Therap Apheres.* (2002) 6:394–98. doi: 10.1046/j.1526-0968.2002.00427.x
52. Khan TZ, Pottle A, Pennell DJ, Barbir MS. The impact of lipoprotein apheresis in patients with refractory angina and raised Lipoprotein(a): objectives and methods of a randomised controlled trial. *Atheroscler Suppl.* (2015) 18:103–8. doi:10.1016/j.atherosclerosissup.2015.02.019
53. Bengsch S, Boos KS, Nagel D, Seidel D, Inthorn D. Extracorporeal plasma treatment for the removal of endotoxin in patients with sepsis: clinical results of a pilot study. *Shock.* (2005) 23:494–500
54. Samtleben W, Bengsch S, Boos KS, Seidel D. HELP Apheresis in the treatment of sepsis. *Artif Organs.* (1998) 22:43–6. doi: 10.1046/j.1525-1594.1998.06011.x
55. Jaeger BR, Goehring P, Schirmer J, Uhrig S, Lohse P, Kreuzer E, et al. Consistent lowering of clotting factors for the treatment of acute cardiovascular syndromes and hypercoagulability: a different pathophysiological approach. *Therap Apheres.* (2001) 5:252–9. doi: 10.1046/j.1526-0968.2001.00350.x

56. Jaeger BR, Labarrere CA. Fibrinogen and atherothrombosis: vulnerable plaque or vulnerable patient? *Herz.* (2003) 28:530- 8. doi: 10.1007/s00059-003-2497-5
57. O'Connor RJ, Preston N, Parkin A, Makower S, Ross D, Gee J, et al. The COVID-19 Yorkshire Rehabilitation Scale (C19-YRS): Application and psychometric analysis in a post-COVID-19 syndrome cohort. *Journal of Medical Virology.* 2022;94(3):1027-34.
58. Sivan M, Parkin A, Makower S, Greenwood DC. Post-COVID syndrome symptoms, functional disability, and clinical severity phenotypes in hospitalized and nonhospitalized individuals: A cross-sectional evaluation from a community COVID rehabilitation service. *J Med Virol.* 2021.
59. Ye S, Sun K, Huynh D, Phi HQ, Ko B, Huang B, Ghomi RH. A computerized cognitive test battery for detection of dementia and mild cognitive impairment: instrument validation study. *JMIR aging.* 2022 Apr 15;5(2):e36825.
60. Wade DT, Wood VA, Heller A, Maggs J, Langton Hewer R. Walking after stroke. Measurement and recovery over the first 3 months. *Scand J Rehabil Med.* 1987;19(1):25-30.
61. Shaffer F, Ginsberg JP. An Overview of Heart Rate Variability Metrics and Norms. *Front Public Health.* 2017;5:258-.
62. Rodstein M, Zeman FD. Postural blood pressure changes in the elderly. *J Chronic Dis.* 1957;6(6):581-8
63. Freeman R, Wieling W, Axelrod FB, Benditt DG, Benarroch E, Biaggioni I, Cheshire WP, Chelimsky T, Cortelli P, Gibbons CH, Goldstein DS. Consensus statement on the definition of orthostatic hypotension, neurally mediated syncope and the postural tachycardia syndrome. *Autonomic Neuroscience.* 2011 Apr 26;161(1-2):46-8.
64. Graham BL, Steenbruggen I, Miller MR, Barjaktarevic IZ, Cooper BG, Hall GL, et al. Standardization of spirometry 2019 update. An official American thoracic society and European respiratory society technical statement. *American journal of respiratory and critical care medicine.* 2019;200(8):e70-e88.
65. Macintyre N, Crapo R, Viegi G, Johnson D, Van der Grinten C, Brusasco V, et al. Standardisation of the single-breath determination of carbon monoxide uptake in the lung. *European Respiratory Journal.* 2005;26(4):720-35.
66. Quanjer PH, Stanojevic S, Cole TJ, Baur X, Hall GL, Culver BH, et al. Multi-ethnic reference values for spirometry for the 3–95-yr age range: the global lung function 2012 equations. *Eur Respiratory Soc;* 2012.
67. Stanojevic S, Graham BL, Cooper BG, Thompson BR, Carter KW, Francis RW, et al. Official ERS technical standards: Global Lung Function Initiative reference values for the carbon monoxide transfer factor for Caucasians. *European Respiratory Journal.* 2017;50(3).
68. Pretorius E, Venter C, Laubscher GJ, Kotze MJ, Oladejo SO, Watson LR, Rajaratnam K, Watson BW, Kell DB. Prevalence of symptoms, comorbidities, fibrin amyloid microclots and platelet pathology in individuals with Long COVID/Post-Acute Sequelae of COVID-19 (PASC). *Cardiovasc Diabetol.* 2022;21:148. doi: 10.1186/s12933-022-01579-5
69. Kell DB, Laubscher GJ, Pretorius E. A central role for amyloid fibrin microclots in long COVID/PASC: origins and therapeutic implications. *Biochem J.* 2022;479:537-559. doi: 10.1042/BCJ20220016
70. Biancalana M, Koide S. Molecular mechanism of Thioflavin-T binding to amyloid fibrils. *Biochim Biophys Acta.* 2010;1804:1405-1412. doi: 10.1016/j.bbapap.2010.04.001

71. Pretorius E, Vlok M, Venter C, Bezuidenhout JA, Laubscher GJ, Steenkamp J, Kell DB. Persistent clotting protein pathology in Long COVID/Post-Acute Sequelae of COVID-19 (PASC) is accompanied by increased levels of antiplasmin. *Cardiovasc Diabetol*. 2021;20:172. doi: 10.1186/s12933-021-01359-7
72. Otto O, Rosendahl P, Mietke A, Golfier S, Herold C, Klaue D, et al. Real-time deformability cytometry: on-the-fly cell mechanical phenotyping. *Nat Methods*. 2015;12(3):199-202, 4 p following
73. Toepfner N, Herold C, Otto O, Rosendahl P, Jacobi A, Kräter M, et al. Detection of human disease conditions by single-cell morpho-rheological phenotyping of blood. *Elife*. 2018;7.
74. Müller P, O'Connell E. Shape-Out version 2.9.2: Graphical user interface for analysis and visualization of RT-DC data sets [Software] <https://github.com/ZELLMECHANIK-DRESDEN/ShapeOut2.2019> [Available from: <https://github.com/ZELLMECHANIK-DRESDEN/ShapeOut2>].
75. Kubánková M, Hohberger B, Hoffmanns J, Fürst J, Herrmann M, Guck J, et al. Physical phenotype of blood cells is altered in COVID-19. *Biophys J*. 2021;120(14):2838-47.

Supplementary Material

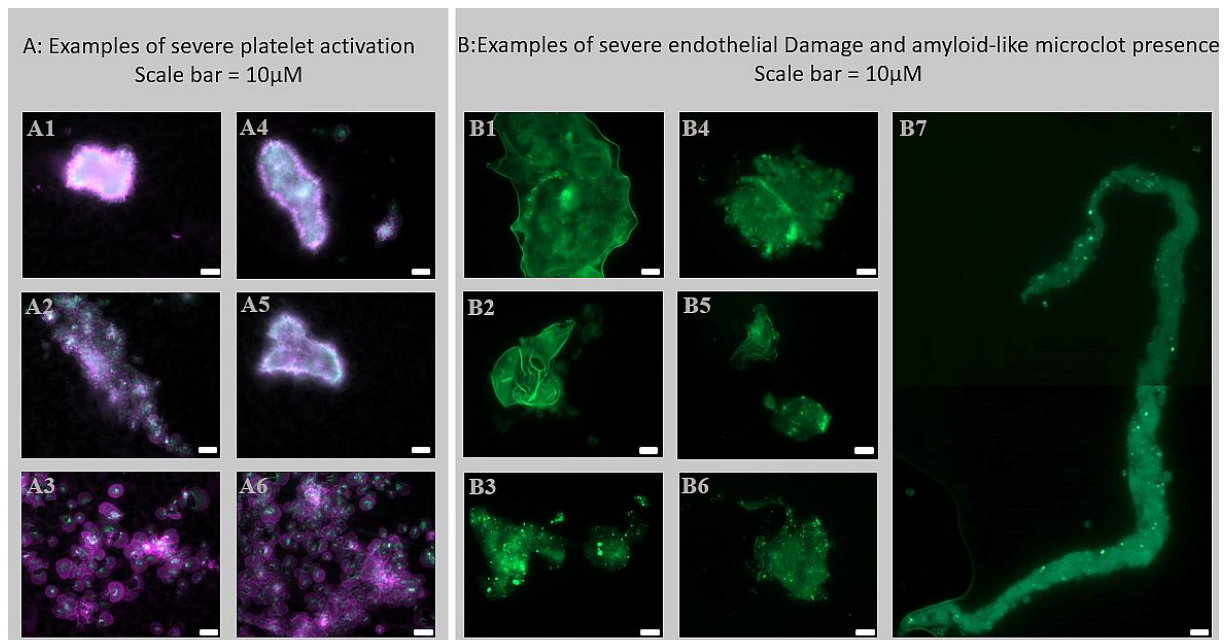


Figure S1. Further illustrations of platelet activation (A) and amyloid-like microclot structures, endothelial damage, plasma protein misfolding, and fibrinogen-like structures (B) in Long COVID and post-COVID-19 vaccination syndrome. A4 has a diameter of approximately 53μM, B1 has a diameter of around 80μM, and B7 has a length of approximately 500 μM (0,5mm), to give a rough indication of the size of these structures in circulation.

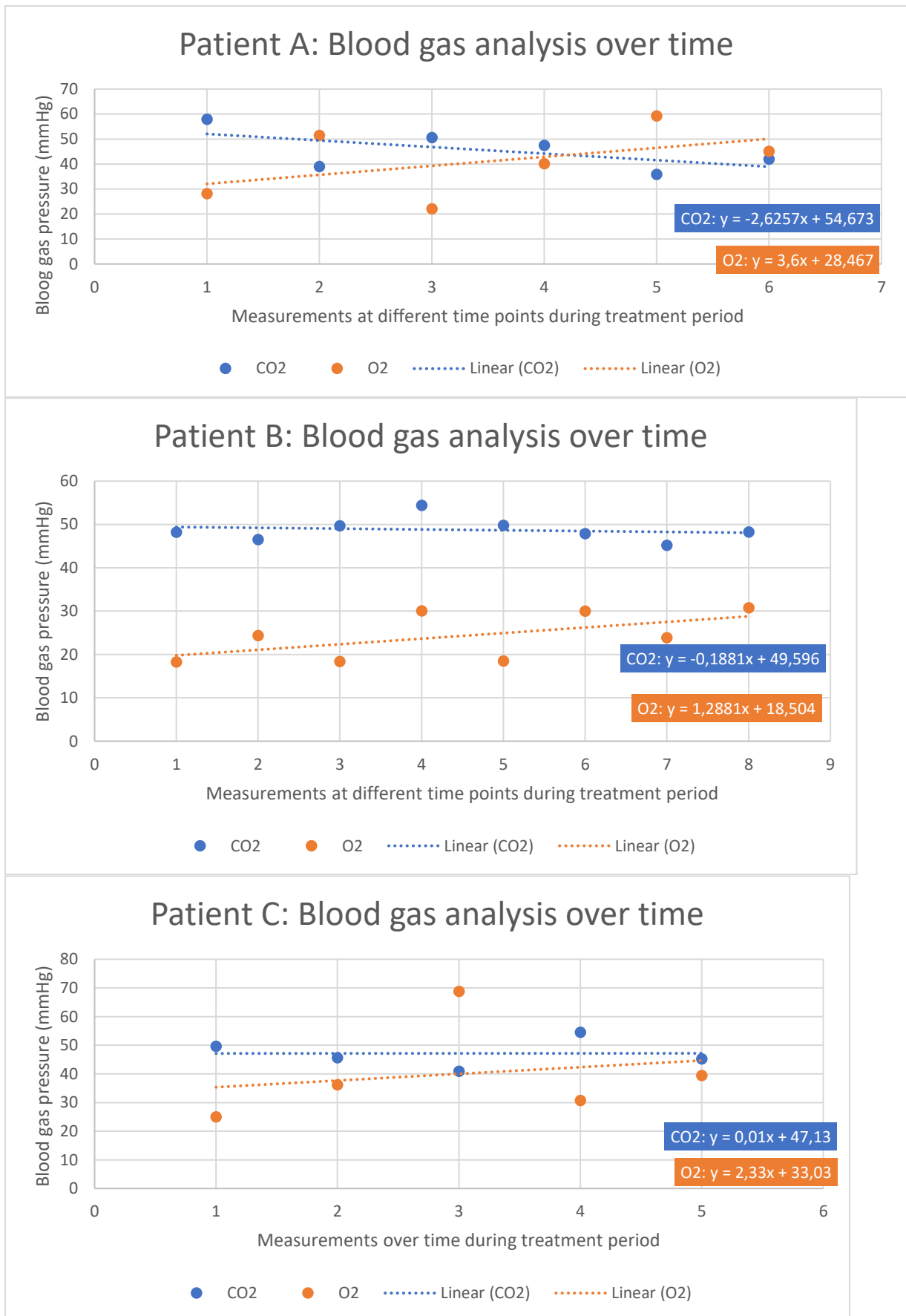


Figure S2. Individual blood gas analysis (pO₂ and pCO₂) of three patients that showcase the typical changes in venous oxygen and carbon dioxide pressure

